Generation of a canine anti-EGFR (ErbB-1) antibody for passive immunotherapy in dog cancer patients.

Singer, Fazekas et al.

Supplementary Figure Legends

Supplementary Fig. S1: Purification of can225IgG.

a: Western Blot analysis of recombinant Protein A purification traces of can225IgG.
Can225IgG did not bind to the recombinant protein A column; antibodies (staining for Fc-regions) were detectable in flow-through (FT) and wash fractions (W1), but not in the eluates (E1-E4). Dog IgG Standard (IgG STD) and untreated cell culture supernatant of can225IgG producing cells (can 225IgG Sup) served as positive controls, bovine serum albumin (BSA) as negative control.

b: Western Blot analysis of recombinant Protein G purification traces of can225IgG.
Can225IgG bound recombinant protein G. The column could deplete transfected CHO-cell culture supernatant, as there is no signal detectable in flow-through and wash fractions (W1), but clear signal in the eluates (E1-E3, minor in E4). Canine IgG Standard served as positive, BSA as negative control.

Supplementary Fig. S2: 10% SDS-PAGE analyzing can225IgG before and after Protein G purification.

Lane 2 and 3 show intact recombinant protein after and prior to purification, respectively.

Supplementary Fig. S3: Flow cytometric assessment of can225IgG binding to cells.

Can225IgG binding towards EGFR was investigated on canine mammary carcinoma cells CF33 and CF41, canine melanoma cell line TLM1, lacking EGFR expression and human mammary carcinoma cell line BT474.

a: Canine CF33 cells could be specifically stained with the generated can225IgG antibody (black line), compared to isotype control staining (grey histogram), difference in mean fluorescence intensity (ΔMFI) = 5.76

b: Canine CF41 cells, ΔMFI = 1.12

c: TLM1 cells lacking EGFR expression display even lower signal than background fluorescence obtained with the isotype control, dog IgG standard, ΔMFI = -6.78

d: Human BT474 cells, ΔMFI = 6.70.

Supplementary Fig. S4: Competitive flow cytometry of can225IgG binding to human or canine EGFR.

a: Surface EGFR expression on canine P114 cells, stained with cetuximab and anti-human IgG (H+L) AlexaFluor® 488 antibodies (black line), compared to isotype control staining (grey histogram), difference in mean fluorescence intensity (ΔMFI) = 14,16

b: surface EGFR expression on human BT474 cells, ΔMFI = 18,05

c: surface EGFR expression on human A431 cells, ΔMFI = 2664,04

d: Competitive flow cytometry measurement of can225IgG binding on canine P114 cells. Can225IgG binds specifically canine EGFR on the surface of canine P114 cells (=100%). Upon incubation with increasing concentrations of soluble human EGFR, Median Fluorescence Intensity (MFI) decreases dose-dependendently, indicating lower affinity of can225IgG for canine than towards human EGFR.

e:Competitive flow cytometry measurement of can225IgG binding on human BT474 cells. Can225IgG binds specifically human EGFR on the surface of human BT474 cells (=100%). Upon competitive incubation with soluble EGFR, no reduction of Median Fluorescence Intensity (MFI) can be detected, even upon molar excess (displayed are mean values ± SEM, n=2).

Supplementary Fig. S5: Immunofluorescence and immuno-histochemical staining of canine mammary carcinoma with can225IgG.

a: Immunofluorescence of EGFR-overexpressing A431 cells. Canine (top left) and human isotype controls (bottom left) showed only background staining on the surface of A431 cells. In contrast, both can225IgG (top right) as well as cetuximab (bottom right) displayed strong, membrane specific staining of ErbB-1 receptors. Original magnifications: x 400.

b: Immunohistochemical staining of canine mammary carcinoma sections. Left: Sections of mammary carcinoma samples, stained with EGFR pharm Dx™ kit, showed strong and complete membrane specific signal for EGFR expression. Middle: Canine IgG Standard as negative control. Right: staining with can225IgG displayed specific EGFR staining, comparable to the FDA-approved diagnostic kit. Original magnifications: x 200.

Supplementary Figure S1; Singer, Fazekas et al.

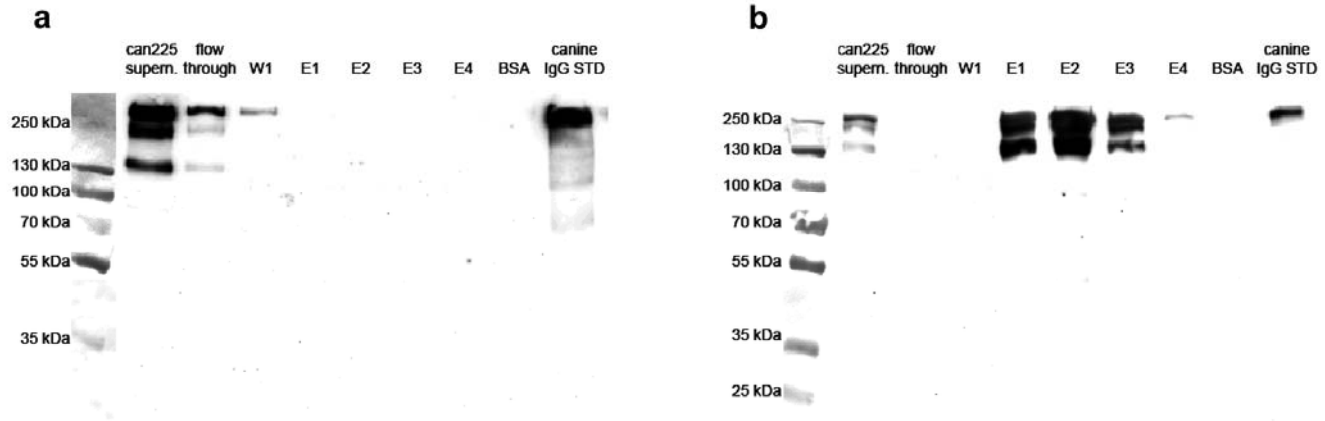

Supplementary Figure S2; Singer, Fazekas et al.

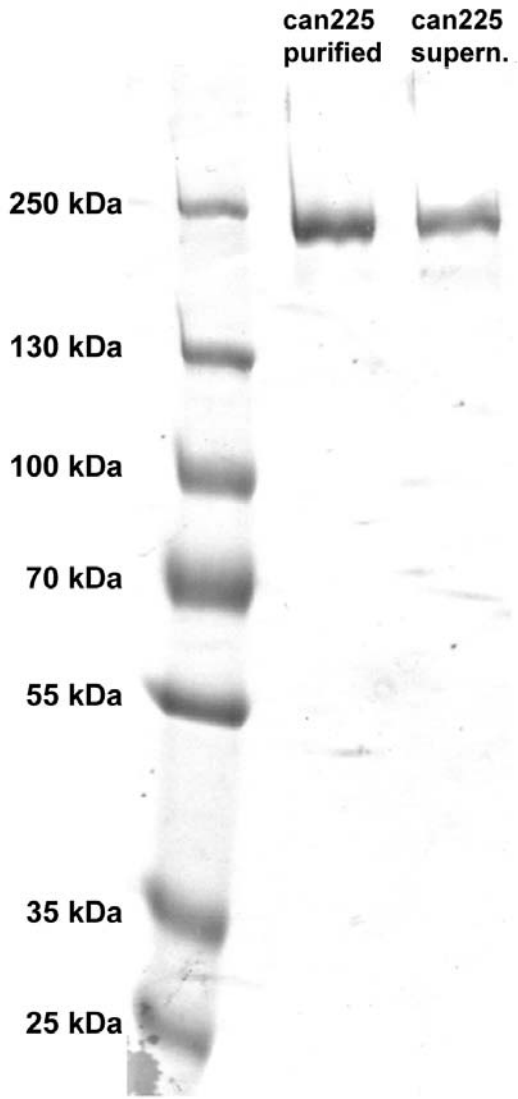

Supplementary Figure S3; Singer, Fazekas et al.

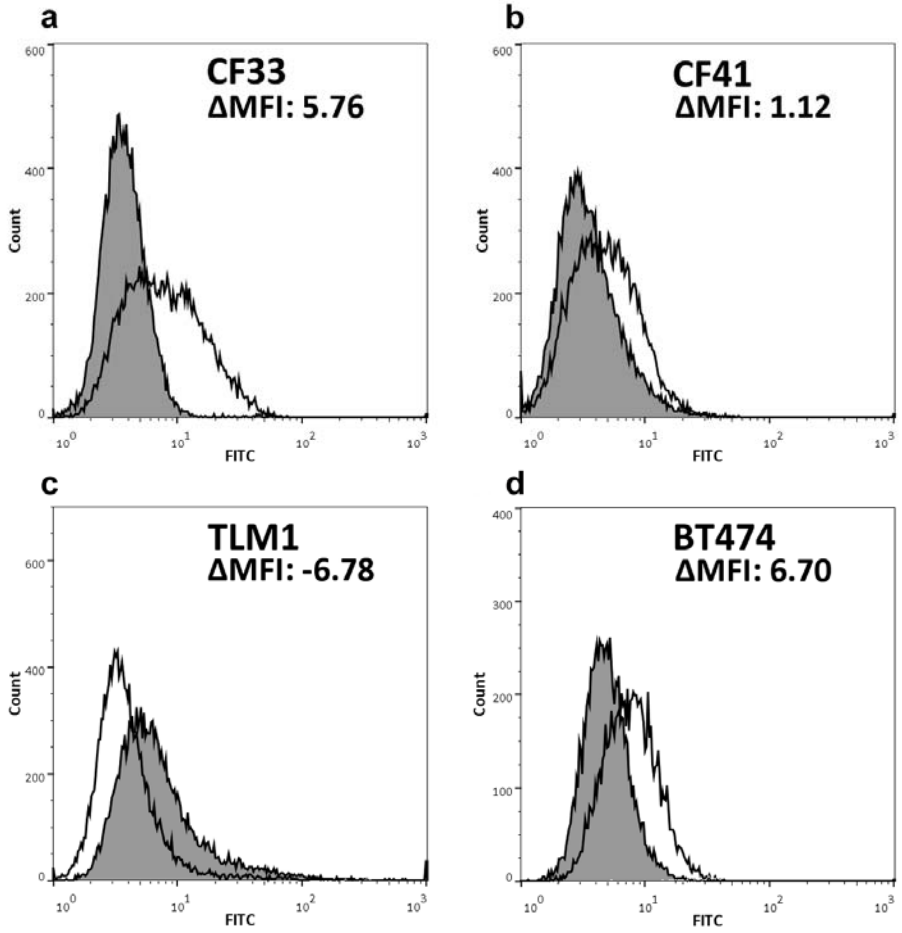

Supplementary Figure S4; Singer, Fazekas et al.

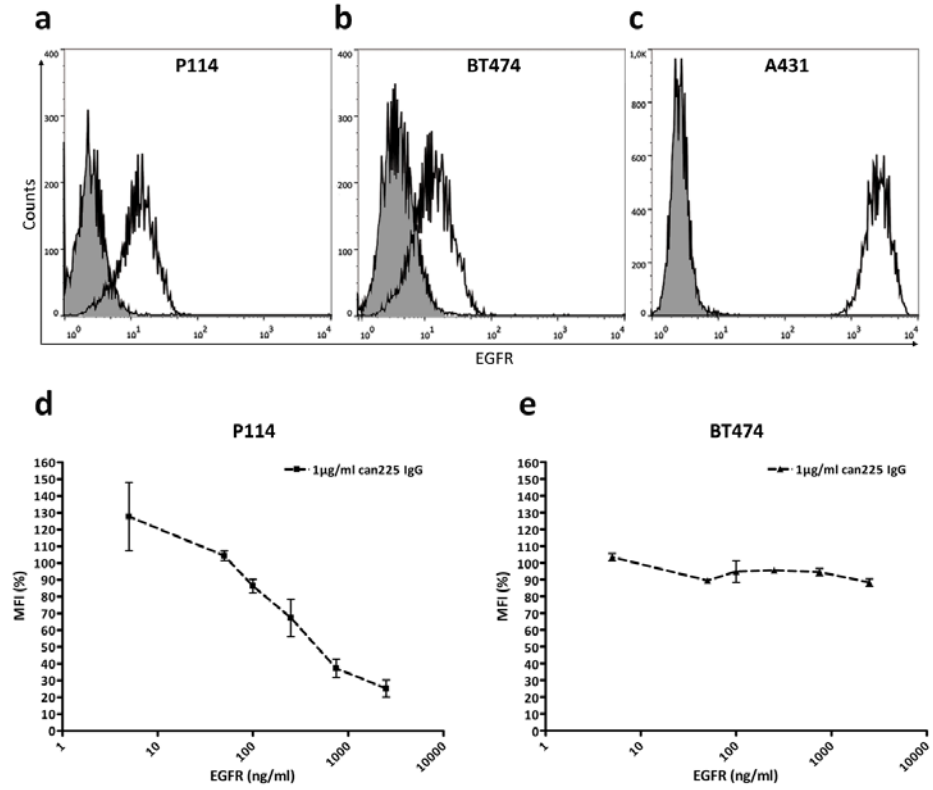

Supplementary Figure S5; Singer, Fazekas et al.

a

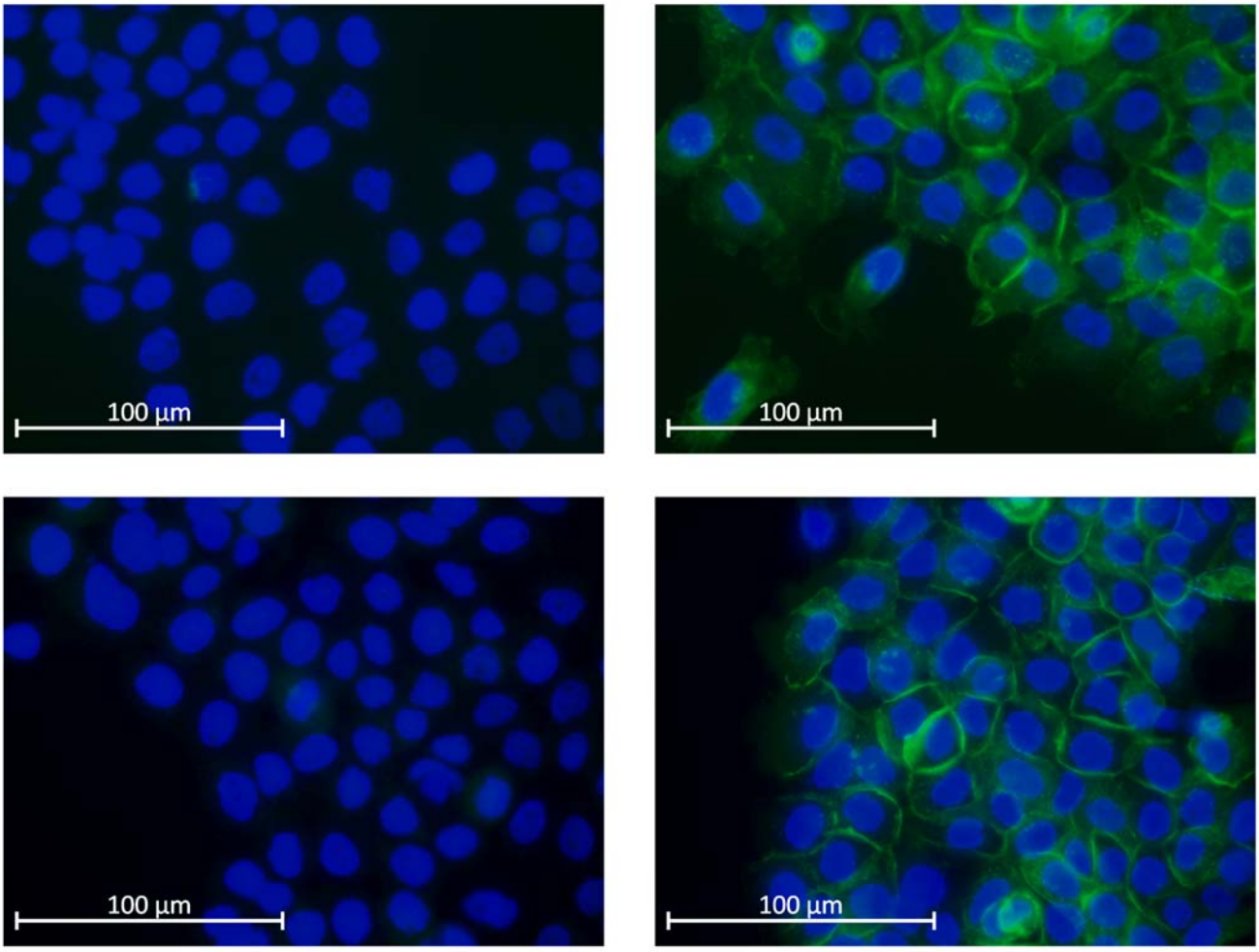

b